

**Charged Synthetic Polystyrene Heterostructures for Charge Trapping and Piezoelectric  
Response**

by  
Chen Chi

A thesis submitted to Johns Hopkins University in conformity with the requirements for the degree of Master of  
Science in Engineering.

Baltimore, Maryland

December, 2018

© Chen Chi 2018

All Rights Reserved

## Abstract

Piezoelectric polymeric material is a comparatively new field of research but may have potential in numerous applications. In this project, we describe a chemical design and synthesis method for a set of polystyrene-based polymers including two crosslinked polymers using free radical polymerization and side-chain functionalization. The synthesized polymers were drop cast on copper plates to fabricate devices with thick films and charged by Corona charging. Surface voltages were tested to illustrate the charge storage capabilities, and  $d_{33}$  coefficients of different films were measured as a manifestation of their piezoelectric responses. We observed that the charge storage capability depended on both the glass transition temperature ( $T_g$ ) and the functional side groups of the polymer while the piezoelectric response depended on charge storage capability as well as the flexibility of the polymers. One of the synthesized polymers showed a remarkably high  $d_{33}$  coefficient of 168 pC/N. Even some of the lower  $d_{33}$  obtained for some polymers of around 70 pC/N are in the upper range for this polymer class.

Advisor: Howard E. Katz

## **Acknowledgements**

My adviser Professor Howard E. Katz and our coordinator Professor James E. West had a significant influence on this essay.

I'd also like to thank Qingyang Zhang, Valerie Rennoll and Ugur Erturun for their help in this project.

Funding by the Department of Energy, Office of Science, Office of Basic Energy Sciences, Materials Chemistry Program, Grant Number DEFG02-07ER46465 is gratefully acknowledged.

# Contents

<b>Acknowledgements</b>	iii
<b>1 Introduction</b>	1
<b>2 Experimental Section</b>	2
2.1 Polymer Synthesis . . . . .	2
2.2 Device Fabrication . . . . .	5
<b>3 Results and Discussions</b>	5
3.1 Polymer Design and Synthesis . . . . .	5
3.2 Device Fabrication . . . . .	7
3.3 Poling and Surface Voltage Measurement. . . . .	8
3.4 Piezoelectric Coefficient ( $d_{33}$ ) Measurements. . . . .	10
<b>4 Conclusion</b>	12
<b>Bibliography</b>	13
<b>Appendices</b>	14
<b>Curriculum Vitae</b>	20

## List of Tables

Table 1. Results of $d_{33}$ measurements. . . . .	11
--	----

## List of Figures

Scheme 1 Synthesis of polymers used in the device fabrication . . . . .	4
Figure 1. Device fabrication process. . . . .	5
Figure 2. Surface voltage of polymer films with respect to time after poling. . . . .	7
Figure A1. $^1\text{H}$ NMR ( $\text{CDCl}_3$ ) spectrum of PS-CF3. . . . .	14
Figure A2. $^1\text{H}$ NMR ( $\text{CDCl}_3$ ) spectrum of PS-AS. . . . .	14
Figure A3. $^1\text{H}$ NMR ( $\text{CDCl}_3$ & MeOD) spectrum of PS-VPh. . . . .	15
Figure A4. $^1\text{H}$ NMR ( $\text{CDCl}_3$ ) spectrum of PS-Si. . . . .	15
Figure A5. $^1\text{H}$ NMR ( $\text{CDCl}_3$ ) spectrum of PS-VBCB. . . . .	16
Figure A6. $^1\text{H}$ NMR ( $\text{CDCl}_3$ ) spectrum of PS-CF3-VBCB. . . . .	16
Figure A7. GPC trace of PS-CF3. . . . .	17
Figure A8. GPC trace of PS-Si. . . . .	17
Figure A9. GPC trace of PS-VBCB. . . . .	18
Figure A10. GPC trace of PS-CF3-VBCB. . . . .	18
Figure A11. DSC plot of PS-CF3. . . . .	19
Figure A12. DSC plot of PS-Si. . . . .	19

# 1. Introduction

Piezoelectric materials have a wide range of applications from ultrasonic imaging for therapeutic purposes to microelectromechanical systems (MEMS) and biosensors. [1] Compared to traditional inorganic materials like lead zirconate titanate (PZT) that have significant disadvantages such as toxicity, high processing temperature and high cost manufacturing capabilities for fabrication [2], polymeric piezoelectric materials show properties that are advantageous for fabrication and application, such as the mechanical flexibility, solubility and less expensive material cost. [3]

Generally, three categories of polymers show piezoelectric properties: bulk piezoelectric polymers, polymer piezoelectric composites and voided charged polymers (VCP). For different categories of piezoelectric polymers, different mechanisms are operative. In bulk piezoelectric polymers, the molecular structure, or more exactly the inherent dipoles and the capability of dipole reorientation through poling result in their piezoelectric behavior. [4] There are two types of polymers in this category: semi-crystalline polymers such as polyvinylidene fluoride (PVDF) [5], polyamides, liquid crystal polymers [4] and Parylene-C [6]; and amorphous polymers such as polyimide[7], polyvinylidene chloride (PVDC)[4] and a set of polystyrene-based polymers that will be discussed in this essay. In polymer piezoelectric composites, or piezocomposite, polymers are embedded with inorganic piezoelectric materials that contribute almost all of the piezoelectric behavior while the polymer part only provides mechanical flexibility. Examples of piezocomposites include PZT/polymer where the composites containing polyurethanes or epoxies are commercially available. In VCP, the piezoelectricity results from the internal gas voids where gas molecules are ionized through poling and charges are implanted on the sides of the voids.[7].

Different from regular piezoelectric materials, the piezoelectric coefficient in VCP depends significantly on the density and shape of voids as well as the type and pressure of gas therein. Modelled as a structure of charges suspended with springs and dampers, another influential factor is the frequency of applied force or electric field.

[8]

In this project, six polystyrene-based polymers are studied: polystyrene (PS), poly(3-trifluoromethyl styrene) (PS-CF<sub>3</sub>), poly(styrene-co-4-pentamethyldisiloxanepropyl styrene) (PS-Si), poly(2-vinylnaphthalene) (PVN), crosslinked PS (XLPS) and crosslinked PS-CF<sub>3</sub> (XLPS-CF<sub>3</sub>). Two of them, PS ( $M_w=192,000$ ,  $T_g\sim 107^\circ\text{C}$ ) and PVN ( $M_w=175,000$ ,  $T_g\sim 135^\circ\text{C}$ ) are purchased from Sigma-Aldrich. The others are synthesized by free radical polymerization initiated with azobisisobutyronitrile (AIBN) and functionalization by organic reactions including side chain modification and crosslinking. The molecular weights of the synthesized PS-CF<sub>3</sub> and PS-Si are measured by gel permeation chromatography (GPC) and the glass transition temperatures ( $T_g$ ) are measured by differential scanning calorimetry (DSC). All the polymers are drop cast on circular copper substrates attached with polytetrafluoroethylene (PTFE) O-rings by epoxy resin to fabricate bilayer devices. Poling are performed by Corona charging at -300V. Then the surface potential change with respect to time and the piezoelectric coefficient ( $d_{33}$ ) are measured. The whole process is simple and low-cost.

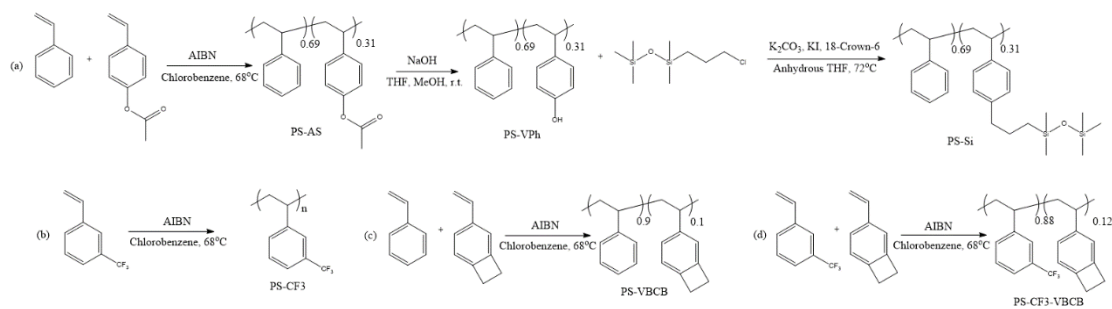
## 2. Experimental Section

### 2.1 Polymer Synthesis

*Synthesis of PS-CF<sub>3</sub>.* A solution of 3-trifluoromethyl styrene monomer and AIBN (3% in weight ratio) in

chlorobenzene (1 mL per gram of monomer) was sealed in a flask and then vacuum-pumped and filled with nitrogen gas each for 5 minutes in three cycles. The solution was stirred under a nitrogen atmosphere at 68°C for 48 hours. After cooling down to ambient temperature, the solution was precipitated in the mixture of 30 mL of water and 120 mL of methanol and stirred for 30 minutes. The precipitated polymer was then dissolved in tetrahydrofuran (THF) and precipitated again in methanol two more times. Afterwards the polymer was dried under vacuum overnight to yield poly(3-trifluoromethyl styrene) in 70% yield. The chemical structures are shown in Scheme 1. The NMR spectra and GPC results are appended in the Appendices. The weight-average molecular weight ( $M_w$ ) is 56700 and the polydispersity index (PDI) is 1.89.

*Synthesis of PS-Si.* The synthesis of PS-Si is a three-step reaction sequence. First a poly(styrene-co-4-acetoxy styrene) (PS-AS) precursor was synthesized with the same procedure as above, except that the monomer was substituted by styrene and 4-acetoxy styrene (35% in weight ratio) and the copolymer was precipitated in 150 mL of methanol. The yield was 75% and the molar ratio of PAS in the copolymer was 31% as shown by  $^1\text{H}$  NMR. Then PS-AS was dissolved THF (5 mL per gram of polymer) and NaOH (5 e.q. of the PAS in the copolymer) was dissolved in methanol (equal amount of THF). The two solutions were mixed in a sealed flask and stirred for 24 hours under ambient conditions. The PAS in the copolymer was hydrolyzed and the solution was precipitated in 150 mL water for 30 minutes for three times. After vacuumed overnight the poly(styrene-co-vinyl phenol) (PS-VPh) was obtained and the yield was 90%. Then, PS-VPh, (3-chloropropyl)pentamethyldisiloxane (4 e.q. of PVPh in the copolymer),  $\text{K}_2\text{CO}_3$  (4 e.q. of PVPh), KI (8 e.q. of PVPh) and 18-crown-6 (0.8 e.q. of PVPh) were mixed in 20 mL of distilled THF. The mixture was vacuum pumped and filled with nitrogen gas each in three cycles and heated to 70°C under a nitrogen atmosphere with stirring for 48 hours. The PS-Si was obtained with a 74% yield



Scheme 1: Synthesis of polymers used in the device fabrication. (a) The three-step synthesis of PS-Si. (b) Synthesis of PS-CF3. (c) Synthesis of PS-VBCB. (d) Synthesis of PS-CF3-VBCB

and the overall yield was 50%. The  $^1\text{H}$  NMR spectra of all the copolymers and the gel permeation chromatogram are listed in the Appendices. The weight-average molecular weight ( $M_w$ ) is 91800 and the polydispersity index (PDI) is 2.32.

*Synthesis of cross-linkable poly(styrene-co-4-vinylbenzocyclobutane).* Cross-linkable poly(styrene-co-4-vinylbenzocyclobutane) (PS-VBCB) was synthesized by the same procedure as described for PS-AS except for the monomer was substituted with styrene and 4-vinylbenzocyclobutane (10% in weight ratio). The obtained cross-linkable PS-VBCB has 10% of PVBCB in molar ratio with a yield of 77%. ( $M_w=44600$ , PDI=1.81)

*Synthesis of cross-linkable poly(3-trifluoromethyl styrene-co-4-vinylbenzocyclobutane).* The synthesis of poly(3-trifluoromethyl styrene-co-4-vinylbenzocyclobutane) (PS-CF3-VBCB) follows the same procedure as described for PS-VBCB except for the monomers used are 3-trifluoromethyl styrene and 4-vinylbenzocyclobutane (10% in weight ratio). The obtained cross-linkable poly(3-trifluoromethyl styrene-co-4-vinylbenzocyclobutane) has 12% of PVBCB in molar ratio with an yield of 77%. ( $M_w=16500$ , PDI=1.93)

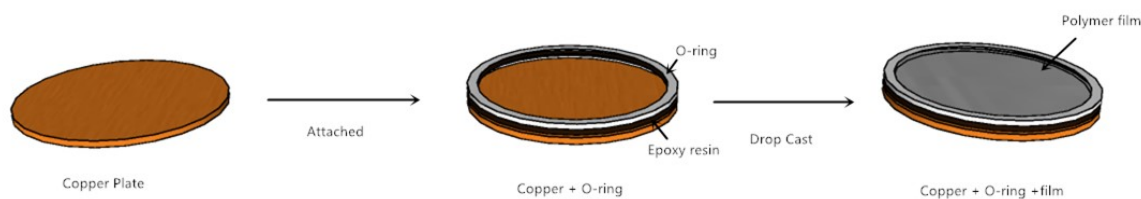


Figure 1. Device fabrication process.

## 2.2 Device Fabrication

All the chargeable devices intended for piezoelectricity measurements were fabricated with the synthesized polymers as in Figure 1. Flat circular copper plates with a diameter of 3.5 cm were cut off from large copper plates and cleaned by sonicating in soap suds, acetone and isopropanol for 15 minutes each. They were dried with a stream of nitrogen gas. Then PTFE O-rings with a diameter of 3 cm were smeared by a 1:1 mixture of the epoxy resin and the hardener and then attached to the copper plates. The substrates were cured overnight. The synthesized polymers were dissolved in 1 mL chlorobenzene (70 mg/mL) separately and filtered with 0.45  $\mu\text{m}$  filters on the tip of 1 mL syringes before drop-cast onto the substrates. The devices were evaporated for 48 hours under ambient conditions. Then the cross-linkable polymer films on the substrates were crosslinked at 200°C for 5 hours under vacuum and then cooled to ambient temperature. Other devices were annealed at 60°C overnight.

## 3. Results and Discussions

### 3.1 Polymer Design and Synthesis

Polystyrene-based materials with different features were designed and synthesized with AIBN initiated free radical polymerization in chlorobenzene. The synthesis of PS-Si was a three-step reaction including polymerization, hydrolysis and postpolymerization functionalization. After the polymerization, PS-VPh was hydrolyzed in a strongly alkaline solution. Then (3-chloropropyl)pentamethyldisiloxane was reacted with the phenol hydroxyl group of PVPh to obtain the required polymer as shown in Scheme 1. Compared to regular PS ( $T_g \sim 107^\circ\text{C}$ [9]), PS-Si had a flexible side chain which contributes to a lower glass transition temperature (around  $60^\circ\text{C}$  as shown in the DSC graph in Appendices).

The siloxane functional group had an unexpected side-effect of being crosslinked. In our first trials 3-chloropropyltris(trimethylsiloxy)silane was chosen to perform the postpolymerization functionalization of the PS backbone. However, even for low ratio (10%) of PVPh in the PS-VPh copolymer the yielded PS-Si was crosslinked severely. The crosslinked polymer was not suitable for device fabrication because it was not soluble and would jam the filter. So (3-chloropropyl)pentamethyldisiloxane was used as it had less siloxane groups and triggered slighter crosslinking. Even with (3-chloropropyl)pentamethyldisiloxane the ratio of PVPh in the PS-VPh copolymer could not exceed 35% or it would still result in severe crosslinking.

PS-CF<sub>3</sub> also had low  $T_g$  of about  $70^\circ\text{C}$  but the substituted group on the benzene group was an electronegative trifluoromethyl group. It was designed to contrast with PS-Si to show the effect of different types of functional groups on the benzene group while  $T_g$  was nearly constant.

Cross-linkable precursors were copolymerized with 4-vinylbenzocyclobutane and styrene or 3-trifluoromethyl

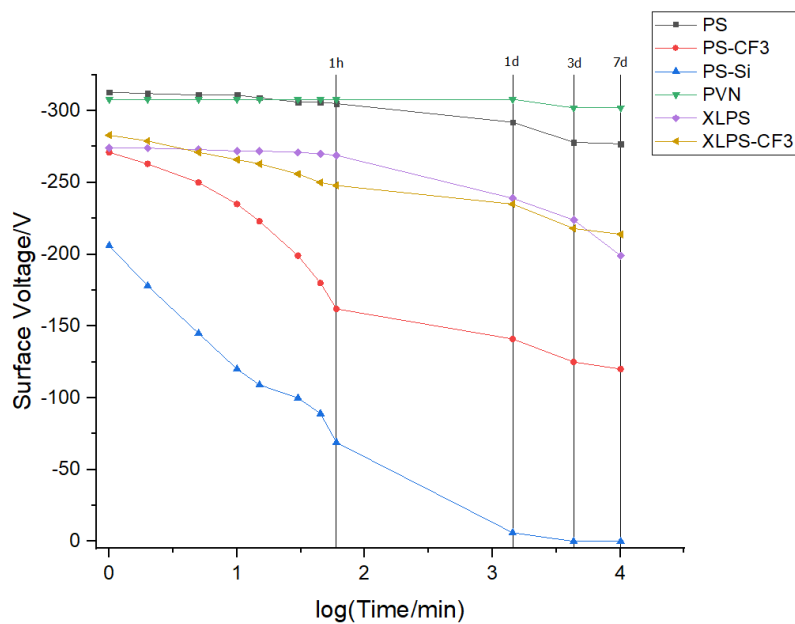


Figure 2. Surface voltage of polymer films with respect to time after poling. The vertical axis scales from 5 to -325 in an opposite way. The horizontal axis is the  $\log_{10}$  value of time with a unit of minute.

styrene. Crosslinking via divinylbenzene subunits, either using benzoyl peroxide or ultraviolet initiation, was not as effective as the cyclobutenostyrene. [10]

### 3.2 Device Fabrication

Different solvents and substrates were tried for device fabrication. Chlorobenzene was confirmed to be a more advantageous solvent than chloroform, dichloromethane (DCM) or toluene to the best of our knowledge. The boiling points of chloroform and DCM were so low that too many bubbles were generated in the film during evaporating. Toluene would cause the fracture of the film.

The main challenge we faced for choosing suitable substrates was to figure out some conductive material that was capable of holding 1 mL of the solutions while remaining as flat as possible. Taking both convenience of processing and cost into consideration, copper was a more advantageous substrate material than silver, iron or gold. For the sake of flatness, instead of rectangular substrates with bent sides which caused unevenness of the substrates and peeling or cracking of the films, circular copper plates were cut off from copper sheets and PTFE O-rings were pasted via epoxy resin, as shown in Figure 1.

In order to obtain a comparably thick film which appeared to show better flexibility, a substantial amount of polymer was drop-cast onto the substrates. The thickness of the films was estimated to be around 100  $\mu\text{m}$  from the density of PS-based materials. After drop-casting, the films of the cross-linkable precursors were heated to obtain XLPS and XLPS-CF3. Other films were annealed to eliminate defects, stress and leftover of solvent in the film.

### 3.3 Poling and Surface Voltage Measurement

In this project, poling was done by Corona charging with SPELLMAN CZE 1000R high voltage power supply and Keithley 248 High Voltage Supply at -300 V and ambient conditions for 1 minute, and the measurement of surface voltage was done with an Isoprobe Electrostatic Voltmeter Model 279 from Monroe Electronics at 1, 2, 5, 10, 15, 30, 45, 60 minutes and 1, 3 and 7 days after charging. The results are shown in Figure 2.

Among all the test samples, PVN showed the best charge storage capability. The surface voltage of PVN hardly changed within one week. PS also showed a remarkably good charge storage capability, decaying less than 10

volts in the first 1 hour after poling and retaining around 90% of its surface charge in a week after poling. Both PVN and PS had higher surface voltage than the poling voltage (-300 V), which may be an indication of the measurement uncertainty. The glass transition temperatures of PS and PVN were 107°C and 135°C, qualitatively showing their low malleability which resulted a comparatively poor attachment to the substrate. In fact, we did observe that PS and PVN were easy to peel from the substrates while other films were impossible to peel. The poor attachment might cause some unobservable air gaps between the films and the substrates that could also lead to the unexpected high surface voltages. In addition, not only was the higher  $T_g$  of PVN seemingly correlated to its good charge storage capability, but also the naphthalene structure with a larger  $\pi$  system was desirable for charge storage because the larger resonance delocalization of the naphthalene ring enabled a better delocalized electron distribution after poling.

In contrast, low  $T_g$  films such as PS-Si and PS-CF<sub>3</sub> showed a significantly worse charge storage capability than the high  $T_g$  ones. The initial surface voltages of the two (-130 V for PS-Si and -271 V for PS-CF<sub>3</sub>) were lower and the decays were more severe. For PS-Si, within the first hour after poling, only 15% of the initial surface voltage was left and no surface voltage was measured 2 days after poling. The PS-CF<sub>3</sub> case was better-approximately 60% and 44% of the surface voltage were retained one hour or one week after poling. From the contrast between the two high  $T_g$  polymer films and the two low  $T_g$  ones it seems that  $T_g$  was a crucial factor for charge storage. High  $T_g$  films showed a consistently better charge storage capability than the low  $T_g$  films in both higher initial surface voltages and lower decay of surface voltages over time. One possible explanation of the observed phenomenon was that for polymers with higher  $T_g$ , the significantly stronger interactions between molecules and the lower free volume would restrict the movement of the polymer chains in the film and trap the

charge.

The obvious difference between the two low  $T_g$  polymer films illustrated that molecular structure could also play an important role in charge storage. The electronegative trifluoromethyl functional group in PS-CF<sub>3</sub> promoted charge storage while the siloxane side chain in PS-Si impaired the charge storage capability.

Compared to their linear counterparts, XLPS and XLPSCF-3 showed different biases in charge storage capability. XLPSCF-3 had a better charge storage capability for the same reason as described above for the higher  $T_g$  polymers because the crosslinked polymers had almost infinite large molecular weights and thus higher  $T_g$  and lower free volume. But in the case for PS, the flexibility was worse so that during crosslinking some stress was generated and resulted in cracks of the films, which made it easier to discharge.

### 3.4 Piezoelectric Coefficient ( $d_{33}$ ) Measurements

The  $d_{33}$  coefficient was measured by a long-stroke vibration exciter which applied a force to a material sandwiched between two fixtures. Stress was applied to one side of a sample from a shaker controlled through LabVIEW. The opposite fixture was attached to a load cell, which measured the corresponding force applied. The shaker could be adjusted to apply various preload forces to the sample. Two leads from the sample collected the charge generated, which was sent to a charge amplifier. All data were collected with a data acquisition system (DAQ) and recorded using LabVIEW. The equipment used is listed: Measurement Specialties Piezo Film Lab Amplifier, Futek Miniature S Beam Load Cell, 10 lb, Brüel & Kjær Charge Amplifier Type 2635, National Instruments BNC-2110, ELECTRO-SEIS APS 113 Shaker, APS 125 Power Amplifier, LabVIEW.

Table 1. Results of  $d_{33}$  measurements.

Sample	Poling date	Date of $d_{33}$ measurement	$d_{33}$ (pC/N)
PS	11/08.18	11/15/18	155
PS-CF3	10/10/18	10/17/18	168
PS-Si	10/10/18	10/17/18	0.46
PVN	10/10/18	10/17/18	66
XLPS	10/10/18	10/17/18	142
XLPS-CF3	11/13/18	11/20/18	78

All the  $d_{33}$  measurements were done with a frequency of 7 Hz, a load amplitude of 2 N and a preload around 7 N after 1 week from poling. The results are shown in Table 1. Combining the surface voltage measurements, molecular structures of the polymers and the  $d_{33}$  measurements, the  $d_{33}$  results were affected by both charge storage capability and the flexibility of the films. First, a comparison between PS, PS-CF3 and PVN showed that even for a film which had an outstanding charge storage capability (PVN), its low flexibility (reflected from the higher  $T_g$ ) would reduce the  $d_{33}$  significantly from 155 pC/N (PS) or 168 pC/N (PS-CF3) to 66 pC/N (PVN). PS-CF3 had a worse charge storage capability than PS as shown in Figure 2 but higher flexibility (an obviously lower  $T_g$ ) so that it even outperformed PS in the  $d_{33}$  measurements. However, PS-Si was the worst sample for  $d_{33}$  because although it was flexible, the charge storage capability was so poor that it could not trap any charge and hardly showed any piezoelectric response (0.46 pC/N).

Taking the two crosslinked polymer films into consideration, the  $d_{33}$  of XLPS (142 pC/N) was smaller than that

of PS (155 pC/N) due to both worse charge storage capability and worse flexibility. However, although the charge storage capability of XLPS-CF3 was better than PS-CF3, its largely worse flexibility predominated in the decrease of  $d_{33}$ . The decrease of  $d_{33}$  from the crosslinking of PS-CF3 was more than 50%, from 168 pC/N to 78 pC/N.

## 4. Conclusion

We synthesized a set of PS-based polymers with multiple representative features such as different flexibility and functional groups. All the films were drop cast on O-ring attached copper plates for surface voltage measurements and piezoelectric coefficient ( $d_{33}$ ) measurements. A better charge storage capability was observed on polymers with higher  $T_g$ , electronegative functional groups and for the flexible polymer, a crosslinking structure. The piezoelectric response of films was influenced by both their charge storage capabilities and flexibilities. Good charge storage capability as well as good flexibility combined in generating a high piezoelectric response which is consistent with charge storage enabling the pressure-induced rearrangement of charges and flexibility influencing the deformation of the films. To combine the two factors, finding novel functional groups that will be helpful for charge storage as well as the decreasing of  $T_g$  is a direction for further progress on this project.

# Bibliography

- [1] W Heywang, K Lubitz, and W Wersing. "Piezoelectricity." *Piezoelectricity Evolution & Future of A Technology* (2008).
- [2] Tadigadapa, S , and K. Mateti . "Piezoelectric MEMS sensors: state-of-the-art and perspectives." *Measurement Science & Technology* 20.9(2009):92001-0.
- [3] Ramadan, Khaled S , D. Sameoto , and S. Evoy . "A review of piezoelectric polymers as functional materials for electromechanical transducers." *Smart Materials & Structures*23.3(2014):33001-33026(26).
- [4] Bryant, Robert G. . *Encyclopedia Of Polymer Science and Technology. Kirk-Othmer Encyclopedia of Chemical Technology*. 2006.
- [5] Jones, Gary D, et al. "Characterization, performance and optimization of PVDF as a piezoelectric film for advanced space mirror concepts." *Journal of Electronic Packaging* 131.1(2005):51-55.
- [6] Kim, Young Hyun, A. Cheng, and Y. C. Tai. "Parylene-C as a piezoelectric material." *IEEE International Conference on Micro Electro Mechanical Systems* 2011.
- [7] Gerhard-Multhaupt, and R. "Less can be more. Holes in polymers lead to a new paradigm of piezoelectric materials for electret transducers." *IEEE Transactions on Dielectrics and Electrical Insulation* 9.5(2002):850-859.
- [8] Bauer, Siegfried, R. Gerhard-Multhaupt, and G. M. Sessler. "Ferroelectrets: Soft Electroactive Foams for Transducers." *Physics Today* 57.2(2004):37-43.
- [9] Blanchard, Louis Philippe , J. Hesse , and S. L. Malhotra . "Effect of Molecular Weight on Glass Transition by Differential Scanning Calorimetry." *Canadian Journal of Chemistry*52.18(1974):3170-3175.
- [10] Alley, Olivia J., et al. "Synthesis, Fabrication, and Heterostructure of Charged, Substituted Polystyrene Multilayer Dielectrics and Their Effects in Pentacene Transistors." *Macromolecules* 49.9(2016):3478-3489.

# Appendices

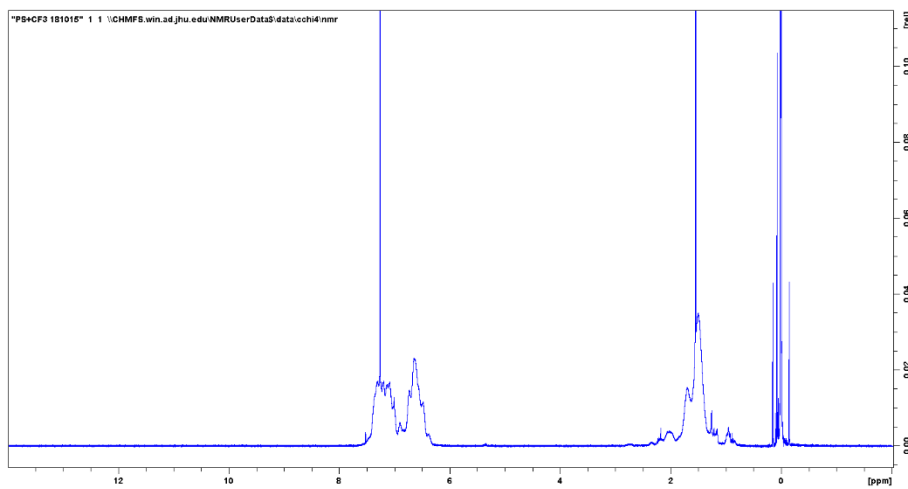


Figure A1. <sup>1</sup>H NMR (CDCl<sub>3</sub>) spectrum of PS-CF3.

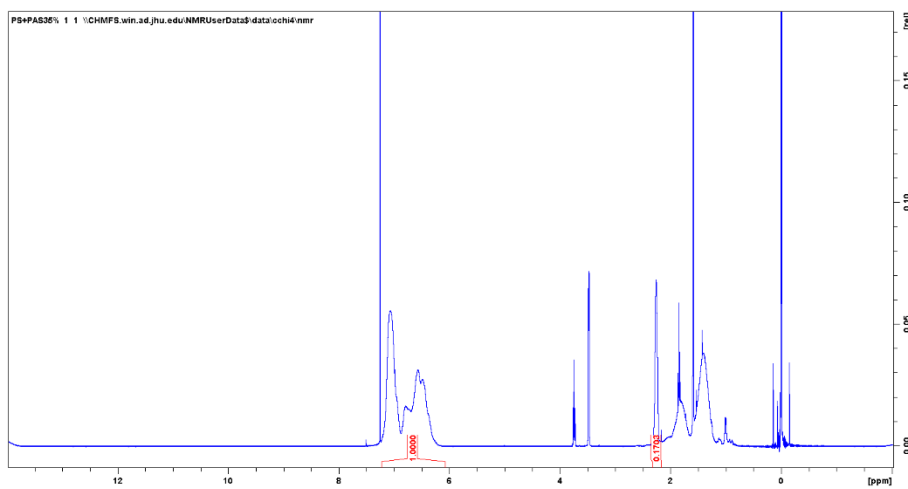


Figure A2. <sup>1</sup>H NMR (CDCl<sub>3</sub>) spectrum of PS-AS.

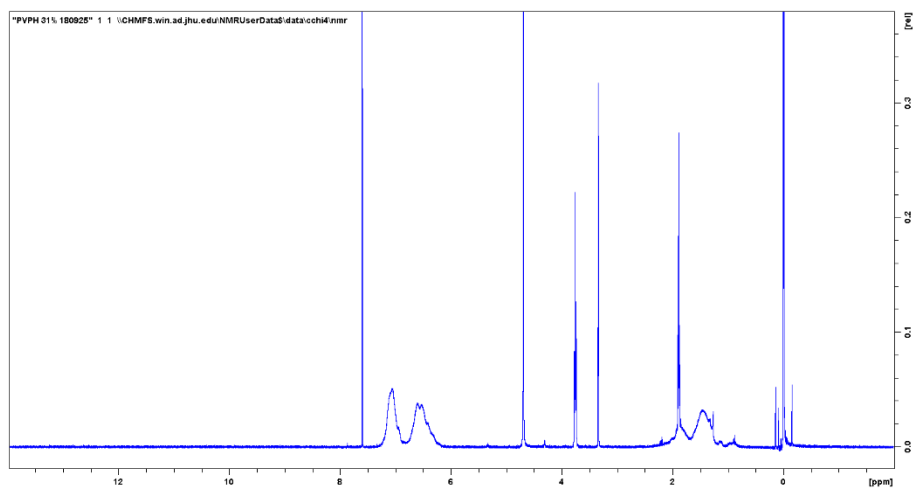


Figure A3. <sup>1</sup>H NMR (CDCl<sub>3</sub> & MeOD) spectrum of PS-VPh.

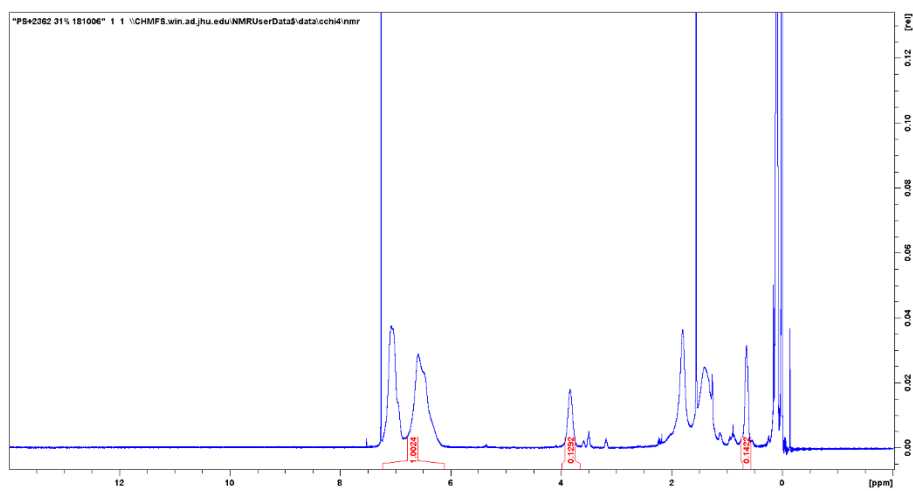


Figure A4. <sup>1</sup>H NMR (CDCl<sub>3</sub>) spectrum of PS-Si.

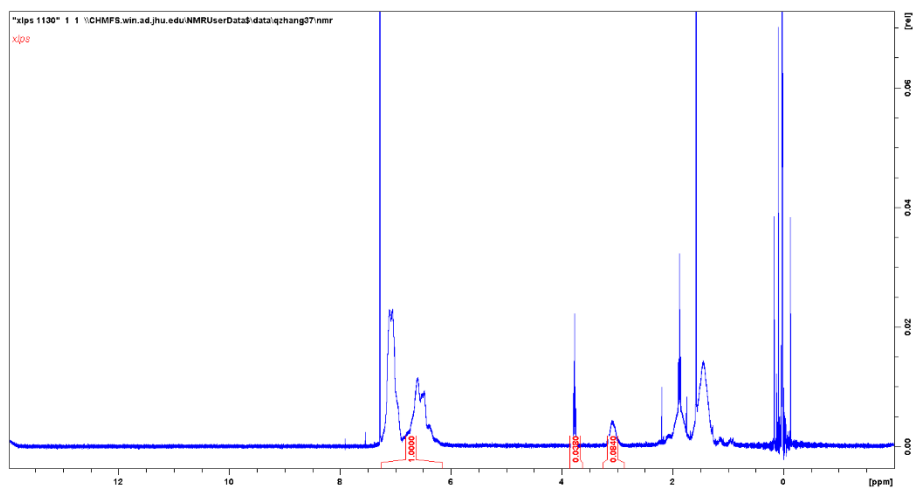


Figure A5. <sup>1</sup>H NMR (CDCl<sub>3</sub>) spectrum of PS-VBCB.

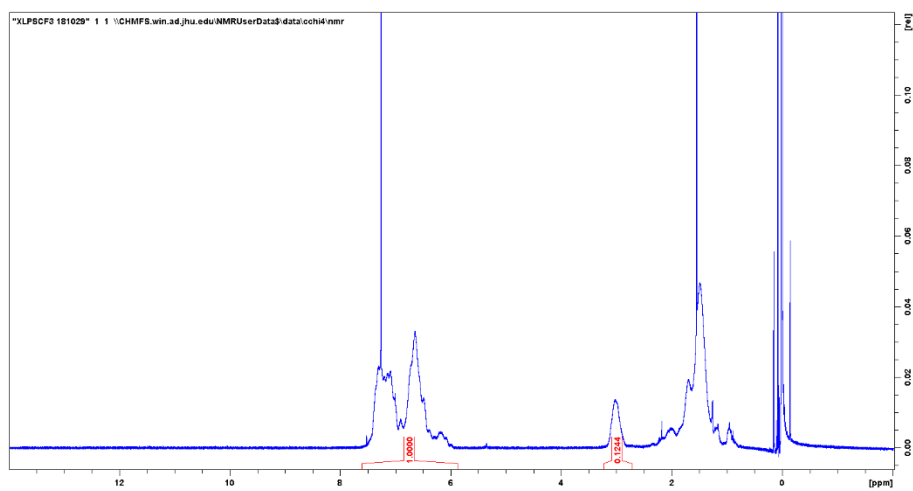


Figure A6. <sup>1</sup>H NMR (CDCl<sub>3</sub>) spectrum of PS-CF<sub>3</sub>-VBCB.

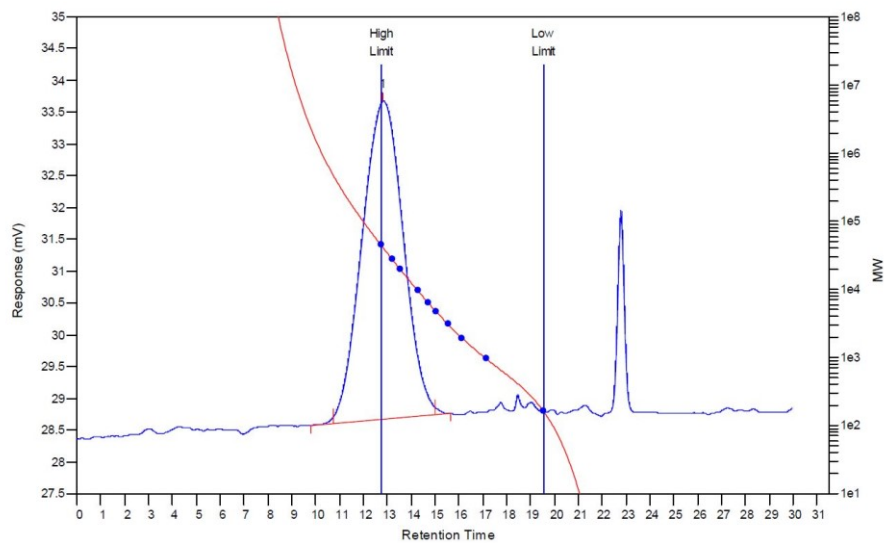


Figure A7. GPC trace of PS-CF3.

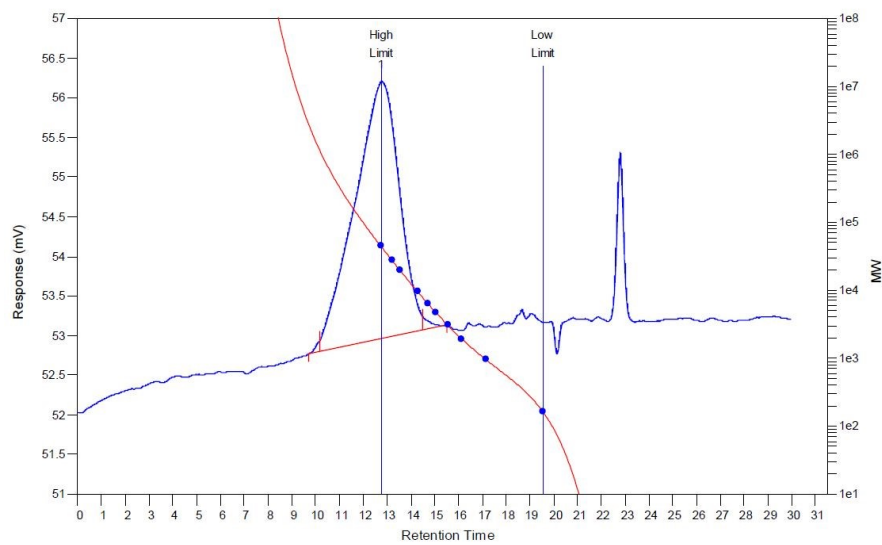


Figure A8. GPC trace of PS-Si.

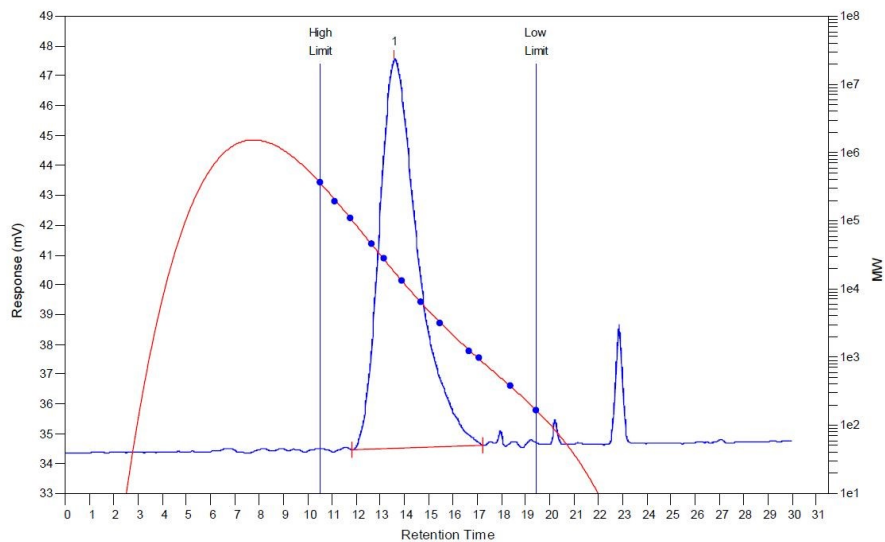


Figure A9. GPC trace of PS-VBCB.

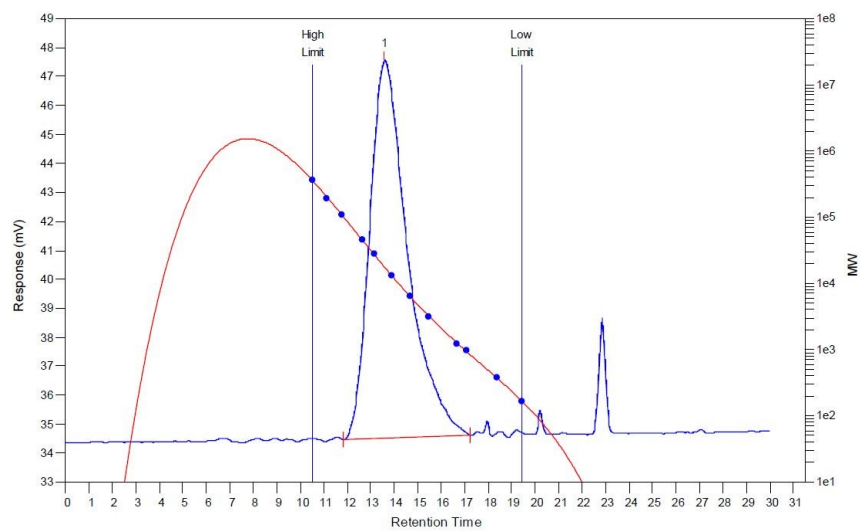


Figure A10. GPC trace of PS-CF3-VBCB.

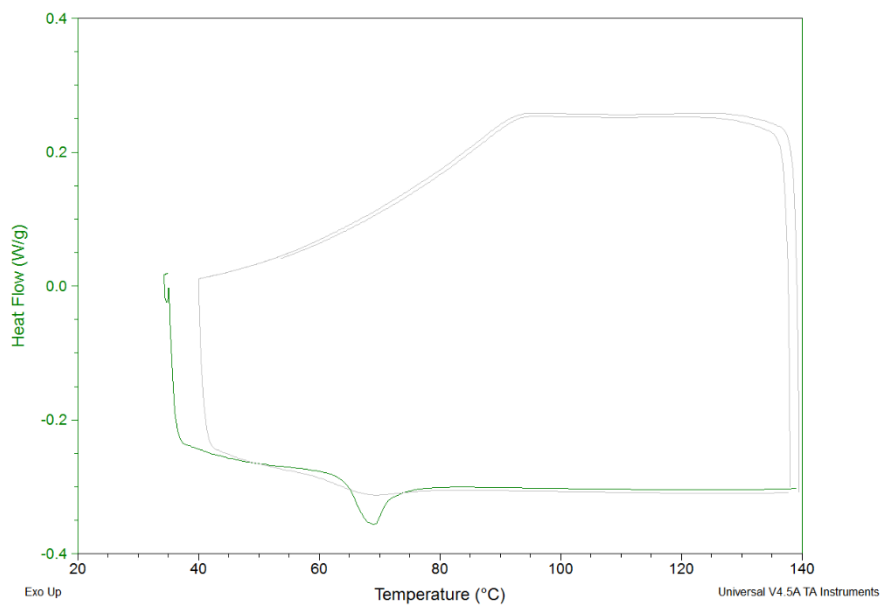


Figure A11. DSC plot of PS-CF3.

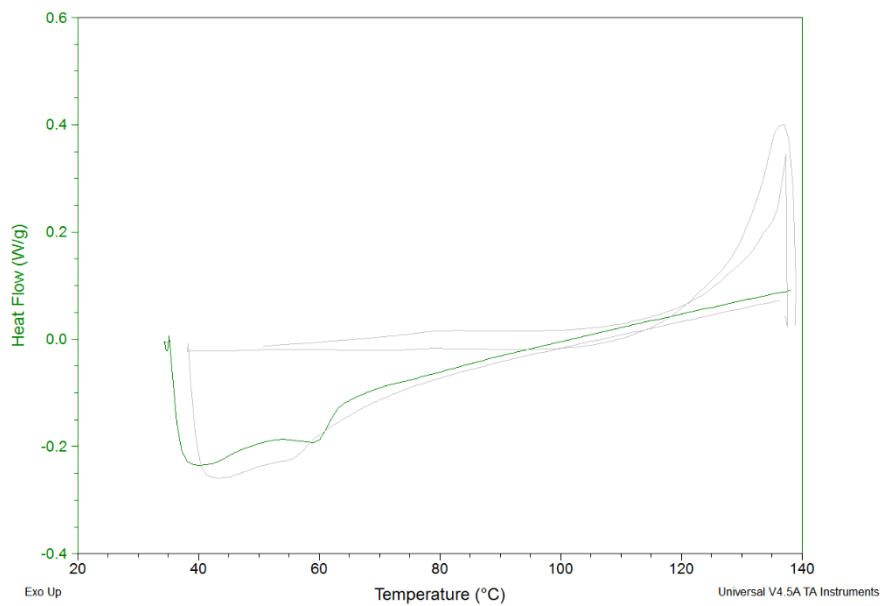


Figure A12. DSC plot of PS-Si.

# Curriculum Vitae

**Chen Chi** (08/09/1994, Weifang, China)

## **EDUCATION BACKGROUND**

---

**Johns Hopkins University (JHU)** 08/2017-12/2018

- Major: Material Science and Engineering
- Expected Degree: Master of Engineering

**Sun Yat-sen University (SYSU)** 09/2013-06/2017

- Major: Macromolecular Material and Engineering
- Degree: Bachelor of Engineering

## **RESEARCH EXPERIENCE**

---

**Charged Synthetic Polystyrene Heterostructures for Charge Trapping and Piezoelectric**

**Response-** Sponsored by Department of Energy 09/2017-Pres.

**Dendritic Side Chain Modification of Polystyrene Based Polymeric Dielectric Material for**

**Charge Storage-**Sponsored by Department of Energy 09/2018-Pres.

**Synthesis and Modification of Hyperbranched Poly(*p*-phenyleneethynylene-*alter-m*-phenyleneethynylene) with Controlled Structure-**Sponsored by National Natural Science

Foundation of China 07/2016-06/2017

**Synthesis of Xanthone Derivative as  $\alpha$ -glucosidase Inhibitors-**Sponsored by National Natural

Science Foundation of China 09/2014-06/2015